



CHORUS

This is the accepted manuscript made available via CHORUS. The article has been published as:

Highly tunable piezocaloric effect in antiferroelectric PbZrO_3

S. Lisenkov, B. K. Mani, J. Cuzzo, and I. Ponomareva

Phys. Rev. B **93**, 064108 — Published 12 February 2016

DOI: [10.1103/PhysRevB.93.064108](https://doi.org/10.1103/PhysRevB.93.064108)

Highly tunable piezocaloric effect in antiferroelectric PbZrO_3

S. Lisenkov,¹ B. K. Mani,¹ J. Cuzzo,¹ and I. Ponomareva¹

¹*Department of Physics, University of South Florida, Tampa, Florida 33620, USA*

Abstract

First-principles-based effective Hamiltonian approach is used to predict the existence of a highly tunable piezocaloric effect in antiferroelectric PbZrO_3 . The high tunability originates from a strong dependence of both the magnitude and sign of the piezocaloric temperature change on the initial temperature and the nature of stress. The linearity of the temperature response to the applied stress allows for the doubling of the efficiency of the basic solid state refrigeration cycle. The large values and high tunability of the piezocaloric effect in antiferroelectrics is traced to the strong coupling between the multiple order parameters that coexist in such materials. An experimental setup for the demonstration of such an unusual effect is proposed.

Caloric effects in functional materials are presently under intense investigation owing to both the discoveries of giant caloric effects in several ferroics [1–9] and their technological promise for solid state refrigeration. The solid state refrigeration is regarded as an energy efficient and environmentally friendly alternative to the conventional refrigeration that utilizes hazardous gases. Caloric effects are defined by either an adiabatic temperature change or by an isothermal entropy change upon application of external fields such as magnetic, electric, or stress fields. The effects in excess of several Kelvins are usually termed as giant which emphasizes the drastic leap from the earlier measurements of just tenths Kelvins [10]. The giant electrocaloric effects of up to 12 K were reported in ferroelectric class/phases of ferroics [8, 9, 11] followed by theoretical predictions of more exotic elastocaloric and multicaloric effects in the same class of materials [12–14]. The latter effects have been recently demonstrated in experiments [15, 16]. The tendency of ferroics to exhibit large multiple caloric effects originates from the strong coupling between ferroelectricity and ferroelasticity that is naturally present in these materials.

As the search for superior caloric materials intensifies it appears fruitful to screen the potential candidates based on their ability to exhibit a strong coupling between the electric (or magnetic) orderings and the structural deformations. Among different ferroics PbZrO_3 is known for its excellent electromechanical response [17]. However, PbZrO_3 is an antiferroelectric and may at first appear as an unlikely caloric material. Indeed, the first direct measurements of the electrocaloric effect in PbZrO_3 yielded only a moderate ΔT of 1.5 K in bulk samples [18]. However, the intrigue behind the discovery was not so much the magnitude of the electrocaloric effect but rather its sign. While a typical ferroelectric warms up under application of the electric field (positive electrocaloric effect), the antiferroelectric PbZrO_3 was found to cool down upon electric field application (negative electrocaloric effect). This unusual discovery prompted further investigations that led to the finding of giant negative electrocaloric effect in antiferroelectric thin films [19]. As the potential of antiferroelectric calorics seems to unfold it provokes a question of whether they could exhibit a large piezocaloric effect. Piezocaloric effect (PCE), also termed as an elastocaloric effect, is associated with a reversible temperature change under the adiabatic application of a stress field and could be as large as the electrocaloric effect in ferroelectric ferroelastics [12, 13]. If such an effect indeed exists in antiferroelectrics then what is its sign? Positive as in ferroelectrics [12], or negative in an analogy with the electrocaloric effect in antiferroelectrics

[18]? Or could the sign of the effect be controlled by the stress field [14]? What is the intrinsic magnitude of the PCE in antiferroelectrics and what is the atomistic mechanism behind the effect? Could the effect be demonstrated in experiments and is it large enough for potential applications? How does the PCE compare to the electrocaloric effect in the same antiferroelectric? These are just a few questions awaiting the answers.

Motivated to address these questions we carry out first-principles-based simulations to investigate the PCE in antiferroelectric PbZrO_3 . Similar computational experiments were previously used to predict the elastocaloric and multicaloric effect in ferroelectrics [12, 13] that have recently received experimental confirmation [15, 16]. The aims of the present study are to: i) predict the (co)existence of large positive and negative PCE in antiferroelectric PbZrO_3 ; ii) reveal the intrinsic features and atomistic origin of the effect; iii) report a high tunability of the PCE by the applied stress and how it may improve the refrigeration cycle; iv) propose an experimental setup to demonstrate the PCE.

We simulate bulk PbZrO_3 that is modeled by a $16 \times 16 \times 16$ supercell periodic along all three Cartesian directions. The total energy of the supercell is given by the first-principles-based effective Hamiltonian of Ref.20. The degrees of freedom for the Hamiltonian include local modes, \mathbf{u} , that are proportional to the dipole moment in the unit cell, oxygen octahedron tilts about pseudocubic axes, $\boldsymbol{\omega}$, that describe oxygen octahedron rotation, and strain variables tensors, η_l , in Voigt notation, that are responsible for the mechanical deformations of a unit cell. Note that the unit cell here refers to a five atom cell of cubic perovskite. The energy of the PbZrO_3 Hamiltonian includes dipole-dipole interactions, short-range interactions, on-site self energies, elastic energy, coupling energy between the degrees of freedom and the interaction between the local modes and electric field and is given in Ref.20. All the parameters of the effective Hamiltonian were computed from first-principles and are reported in Ref.20. The Hamiltonian correctly reproduces many of the electrical and thermodynamical properties of PbZrO_3 [20]. In particular, it accurately predicts the antiferroelectric phase transition and the dipole pattern associated with it, electric hysteresis loops, and the PbZrO_3 behavior under pressure. The computational specific heat at room temperature is $316 \text{ J/K} \cdot \text{kg}$ which compares well with the experimental values of $330\text{-}340 \text{ J/K} \cdot \text{kg}$ [8, 21]. The latent heat of the phase transition in computations is 7.2 kJ/kg which is within the range of the experimental values of $5.0\text{-}12.7 \text{ kJ/kg}$ [21–23]. The thermal expansion coefficient in the antiferroelectric phase and in the absence of stress is $(12.9 \pm 0.8) \cdot 10^{-6} \text{ K}^{-1}$. This com-

compares well with the thermal expansion coefficient of $(13.1 \pm 0.7) \cdot 10^{-6} \text{ K}^{-1}$ computed using the experimental data from Ref.24. Above the Curie point and under zero stress the thermal expansion originates from the unharmonicity of the interatomic potential (mechanical deformation potential in the language of the effective Hamiltonian) which we neglect in the present simulations. Experimentally the thermal expansion coefficient above the Curie point has a relatively small value of $(6.9 \pm 1.1) \cdot 10^{-6} \text{ K}^{-1}$. In our simulations the thermal expansion above the Curie point originates entirely from the applied stress and, therefore, provides a lower estimate for the PCE.

Prior to PCE computations, the simulated sample was annealed from 1200 K to 5 K in steps of 5 K using the canonical Monte Carlo simulations. Thus equilibrated supercells were used in simulations of the piezocaloric effect in the framework of the adiabatic Monte Carlo approach proposed in Refs.12 and 25. In such an approach the caloric change in temperature is computed during the application (or removal) of the stress field under adiabatic conditions. It closely models the direct method for caloric effect measurements [26] and does not require the use of either Maxwell relations or other thermodynamical relations. Direct computations allow us to study both the first-order and the second-order phase transitions, reversible and irreversible processes, and stable and metastable phases. It naturally captures the temperature dependence of the heat capacity. The method was previously found to agree well with experiments for both electrocaloric [25, 27] and piezocaloric [12, 15] effects. Technically, the normal uniaxial stress field, σ , in the range of -2 GPa to 2 GPa was simulated. The stress field was chosen to act either on [100], or [010], or [001] crystallographic planes. In Voigt notation the corresponding components of the stress tensor are σ_1 , or σ_2 , or σ_3 , respectively. In each simulation the stress field was slowly applied and then removed at a rate of 2 kPa per one Monte Carlo sweep. The temperature and structural properties were computed at each Monte Carlo sweep and then averaged over 10,000 Monte Carlo sweeps.

Before we present our computational data for the PCE it is imperative to discuss how the applied stress affects the equilibrium phases of PbZrO_3 . Fig.1 gives the dependencies of the antiferroelectric (AFE), antiferrodistortive (AFD) and strain order parameters on the temperature under zero stress (red curves) and in the presence of the σ_2 stress (all the other curves). The magnitudes of AFE and AFD order parameters are computed as follows: $|AFE| = \sqrt{\langle u_x(\Sigma_2) \rangle^2 + \langle u_y(\Sigma_2) \rangle^2 + \langle u_z(\Sigma_2) \rangle^2}$, where the averages are associated with Σ_2 point of the Brillouin zone. $|AFD| = \sqrt{\langle w_x \rangle^2 + \langle w_y \rangle^2 + \langle w_z \rangle^2}$. All order

parameters are reported relative to the computational lattice constant of cubic PbZrO_3 . Under stress-free conditions the simulated sample undergoes a single phase transition from a paraelectric cubic phase to an antiferroelectric orthorhombic phase with the AFE and AFD order parameters aligned along $[1,0,-1]$ and $[-1,0,1]$ directions of the parent cubic structure (orthorhombic a -axis), respectively. The stress has a pronounced effect on the magnitude of all order parameters as well as the Curie point. In particular, in the AFE phase both the AFE and AFD order parameters are weakened by the tensile (positive) stress and enhanced by the compressive (negative) stress. The same observation holds for the η_2 component of the strain tensor. Consequently, the Curie point is reduced under the tensile stress and increased under compressive stress. Such sensitivity of the structure to the external stress is suggestive of a strong piezocaloric response which relies on the possibility to influence the structural order by the applied stress. Under compressive stress the Clausius-Clapeyron equation, $\frac{\Delta T_C}{\Delta \sigma} = -\frac{\Delta \eta T_C}{L \rho}$, is satisfied. In the latter equation T_C is the Curie temperature, $\Delta \eta$ is the change in strain at the phase transition, L and ρ are the latent heat and density, respectively. From computations $\frac{\Delta T_C}{\Delta \sigma} = -37 \pm 5$ K/GPa, while the estimate from the Clausius-Clapeyron equation gives the value of -51 K/GPa. The negative sign indicates the increase in T_C with the increase in magnitude of compressive stress. Tensile stress induces metastable states (with AFE order parameter pointing along $[101]$ pseudocubic direction) which transition irreversibly to stable states (with AFE order parameter pointing along $[110]$ or $[011]$ pseudocubic direction) in the vicinity of the Curie point. The irreversible nature of this phase transition prohibits application of the Clausius-Clapeyron equation in case of tensile stress. Note that in the AFE phase the structure is much less sensitive to either σ_1 or σ_3 stresses which explains why we do not present the data for those stresses.

Having established the effect of the external stress on the structural distortions in PbZrO_3 we present the computational data for the PCE in this antiferroelectric. Fig.2(a) gives the dependence of the piezocaloric temperature change, ΔT , on the applied stress for a few selected temperatures. Immediately we notice that very large ΔT can be achieved by the application of large stress fields which suggests a strong piezocaloric response. Another striking feature is the linearity of the piezocaloric response below the Curie point (946 K in computations) that gives rise to the change in the sign of the piezocaloric ΔT as the stress changes from compressive to tensile. There are two important consequences to this prediction. First of all, it indicates that both positive and negative PCE can coexist in the

same antiferroelectric. Secondly, it suggests the possibility of controlling the sign of ΔT by the sign of the applied stress that could potentially double the efficiency of the refrigeration cycle as shown in the inset to Fig.2(b). Note, that similar strategy was previously suggested to enhance the electrocaloric ΔT [25]. Finally, we note a strong dependence of both the magnitude and sign of the PCE on the temperature. In particular, while below the Curie temperature the sign of the PCE is controlled by the sign of the applied stress, above the Curie point PCE remains positive for all stresses considered.

To elucidate the origin of such unusual findings we take advantage of the atomistic picture available from our computations. Fig.2(b)-(d) quantifies how the structural order parameters respond to the applications of stress. The change in the order parameters is reported relative to their stress-free values to facilitate the comparison. Several important features are immediately revealed. Firstly, we notice that all three order parameters experience simultaneous, rather large changes that are comparable in magnitude. Secondly, we notice that the change in the strain shows only a weak dependence on the temperature, while the change in the magnitude of the AFE and AFD order parameters follow the temperature evolution of $\Delta T(\sigma)$ from Fig.2(a) rather closely. To elucidate the change in the stress dependence of the AFE order parameter with temperature we recall that this order parameter is coupled to stress via piezoelectric response of the local electric dipoles. Since piezoelectric constants typically exhibit strong temperature dependence the response of the AFE order parameter to stress is also temperature dependent. Similar argument applies to the stress dependence of the AFD order parameter. Finally, we note that the sign of the PCE is largely determined by the change in the magnitude of the AFE and AFD order parameters. If the magnitude of this order parameter decreases the structure becomes less ordered which leads to an increase in the configurational, or structural, entropy. Since the total entropy must be conserved this results in a decrease in the thermal entropy and cooling of the sample. When the magnitude of this order parameter increases, the response is just the opposite and the sample's warming occurs. Based on the atomistic analysis we conclude that the PCE is set into action by the mechanical deformation under the applied stress. The deformation triggers rather large changes in the localized structural distortions (such as AFE and AFD distortions) owing to a strong coupling between the lattice instabilities and the elastic strain. The drastic structural changes result in a considerable entropy flow between the structural ordering and thermal vibrations that gives rise to large PCE. In other words, the PCE in

the antiferroelectric PbZrO_3 is a cooperative action of multiple structural distortions driven by the mechanical deformations. It is worthwhile to note that once such cooperation is destroyed (well above the Curie point) the PCE dramatically weakens.

Once the mechanism responsible for the rather unusual PCE effect in PbZrO_3 is established it is imperative to understand how it plays out in a wider range of temperatures. Fig.3 gives the computational data for the piezocaloric ΔT as a function of temperature. As expected for a cooperative phenomena the PCE reaches its largest values in the vicinity of the Curie point. Below the Curie point the comparison of $\Delta T(T)$ obtained under tensile and compressive stresses confirms that the sign of the piezocaloric ΔT is uniquely determined by the nature of the stress. The robustness of the effect in a very wide range of temperatures is attractive for potential applications.

We also studied application of both compressive and tensile stresses along [100] and [001] pseudocubic directions. These are the directions associated with the nonzero components of the antipolar vector in the AFE phase. In the paraelectric phase the results are very similar to the ones reported in Fig.3 as expected from the symmetry considerations. In the AFE phase, however, the PCE is much smaller as compared to the effect that can be achieved by applying the stress along the orthorhombic c -axis. A rather small piezocaloric ΔT in this case is due to the fact that the AFE PbZrO_3 is much less sensitive to the external stresses that act in the ab orthorhombic plane.

The paraelectric to antiferroelectric phase transition in PbZrO_3 is of the first-order. It is imperative to estimate the piezocaloric ΔT at the first order phase transition. Fig.4 shows a few representative $T(\sigma)$ curves in the vicinity of the Curie point. Under tensile stress the first-order phase transition (indicated by an arrow in Fig.4(a)) is irreversible and, therefore, cannot be used for PCE harvesting. Note that in Fig.3 we do not report the PCE for stresses greater than the ones associated with the irreversible phase transition. Under compressive stress there is a reversible jump in the temperature of about 9 K at the point of the first-order phase transition (indicated by an arrow in Fig.4(b)). From thermodynamics the piezocaloric ΔT at the first-order phase transition can be estimated with the help of the Clausius-Clapeyron equation and the relation $\Delta T = \frac{T\Delta S}{C}$ [28], where ΔS is the entropy change and C is the heat capacity. We obtain $\Delta T \approx \frac{T_C}{\rho c} \frac{d\sigma}{dT_C} \Delta\eta$ or $\Delta T \approx L/c$. Note that c is the specific heat at the Curie point. The above expressions yield 8 K and 6 K, respectively. It is important, however, to realize that the approximate relationships

for ΔT provide only crude estimates due to a very fast variation of the heat capacity in the vicinity of transition temperature. Using the experimental values for L and c [21] we get the estimate of $\Delta T \approx 16$ K. However, this value is too large to assume a constant heat capacity and, therefore, should be used with caution. Nevertheless, the estimate provides an experimental validation for our computational data. Away from the Curie point (Fig.4(c)) the temperature changes continuously suggesting that the first-order phase transition does not contribute to the PCE.

We have also estimated piezocaloric ΔT from the Maxwell equation $\Delta T = - \int_0^\sigma \frac{T}{c\rho} \left(\frac{\partial \eta}{\partial T} \right)_\sigma d\sigma$ (the indirect approach). The results are given in Fig.5. We notice that this method substantially underestimates the piezocaloric ΔT at the Curie point as it does not take into account the entropy change at the first-order phase transition. Indeed the underestimation of the peak ΔT is about 13 K in agreement with the ΔT of 9 K due to the first-order phase transition. The Maxwell equation can also be used to estimate the PCE due to an elastic heating from experimental data. Writing $\eta = \eta_{\sigma=0} + s\sigma$, where s is the elastic compliance, we obtain $\Delta T \approx -\frac{T}{c\rho} \left[\left(\frac{\partial \eta}{\partial T} \right)_{\sigma=0} \sigma_{max} + \left(\frac{\partial s}{\partial T} \right)_{\sigma=0} \frac{\sigma_{max}}{2} \right]$. Using $T = 500$ K, $c = 330$ J/K·kg, $\rho = 8.3$ g/cm³, $\left(\frac{\partial \eta}{\partial T} \right)_{\sigma=0} = 9.9 \cdot 10^{-6}$ K⁻¹ (average of the cubic and orthorhombic phases), $\left(\frac{\partial s}{\partial T} \right)_{\sigma=0} = 2.5 \cdot 10^{-14}$ m²/N·K (estimated from Ref.29), and $\sigma_{max} = 2$ GPa we obtain $\Delta T \approx 13$ K which agrees well with our computational data in Fig.3 away from the phase transition. At the phase transition this value is augmented by 16 K due to the latent heat of the phase transition yielding the experimental estimate of 29 K for the maximum PCE in PbZrO₃. This compares well with our computational value of 39 K under compressive stress (see Fig.3).

To put our findings into perspective we compare the PCE predicted in this work with the relevant caloric effects from the literature in Table I. The second column in the Table reports the room temperature caloric effects. We notice that our predicted value of -1.1 K/GPa compares well with the experimental value of 1.0 K/GPa for PCE [15] and barocaloric [6, 30] effects in other high-performance materials. Furthermore, the room temperature PCE in PbZrO₃ is comparable with the PCE in ferroelectrics (BCZTO ceramics, BST, PbTiO₃, BaTiO₃). The third column in Table I reports the maximum values for different caloric effects and the associated temperature at which the values are achieved. Here we find that PCE in PbZrO₃ (14.5 K/GPa at 523 K) is within the upper boundary of the reported range (6 to 17.5 K/GPa). We also added the values for the electrocaloric effect in PbZrO₃

TABLE I. Piezocaloric, barocaloric, and electrocaloric effects (abbreviated as PCE, BCE, and ECE, respectively) from the literature and this work.

Effect	Near RT value		Max. value	Material	Method	Reference
PCE	$\Delta T/\Delta\sigma$	1.0 K/GPa	6.0 K/GPa (at 335 K)	BCZTO ceramics	exper.	[15]
PCE	$\Delta T/\Delta\sigma$	6.0 K/GPa	9.0 K/GPa (at 250 K)	BST	theory	[12]
PCE	$\Delta T/\Delta\sigma$	3.5 K/GPa	17.5 K/GPa (at 640 K)	PbTiO ₃	theory	[13]
PCE	$\Delta T/\Delta\sigma$	0.8 K/GPa		BaTiO ₃	theory	[14]
PCE	$\Delta T/\Delta\sigma$	-1.1 K/GPa	14.5 K/GPa (at 523 K ^a)	PbZrO ₃	theory	this work
BCE	$\Delta T/\Delta p$	16.7 K/GPa		Ni-Mn-In alloy	exper.	[5]
BCE	$\Delta T/\Delta p$	1 K/GPa	6 K/GPa (at 270 K)	Gd ₅ Si ₂ Ge ₂	exper.	[30]
BCE	$\Delta T/\Delta p$	< -1 K/GPa	-11.3 K/GPa (at 240 K)	La-Fe-Si-Co compound	exper.	[6]
ECE	$\Delta T/\Delta E$	-11 K·cm/MV	-18 K·cm/MV (at 370 K)	PbZrO ₃	exper.	[18]
ECE	$\Delta T/\Delta E$	-14 K·cm/MV	15 K·cm/MV (at 500 K)	PLZT2/95/05	exper.	[19]

^a The computational temperature is rescaled to correct for the Curie point overestimation.

since they may be helpful to estimate the overall performance of this material. Under the experimentally realizable stress of 0.25 GPa [15] the room temperature piezocaloric ΔT is 0.3 K while the maximum value is 3.6 K. Application of both positive and negative stress in the same cycle could potentially double these values to 0.6 K and 7.2 K, respectively. The room temperature value of 0.3 K is comparable to the electrocaloric ΔT in the same material under an applied electric field of 80 kV/cm [18] which may open even more avenues toward the enhancement of the caloric ΔT . Further improvements may be possible through alloying or doping of PbZrO₃.

To achieve the required compressive and tensile stresses experimentally one can utilize a bending setup sketched in Fig.6. In such a setup a thin layer of PbZrO₃ is deposited on top of a substrate. Bending of the substrate creates tensile or compressive stress in the PbZrO₃ layer. From the mechanics of beam bending we estimate that achieving 1 GPa compressive or tensile stress in a micron thick PbZrO₃ film deposited on a few micron thick SrTiO₃ substrate requires creating a bending radius of 45 microns. There is compelling experimental evidence that PbZrO₃ films could withstand a mechanical stress of up to 2.5 GPa [31].

In summary, we studied the intrinsic PCE in an antiferroelectric PbZrO_3 using first-principles-based effective Hamiltonian approach. Our computations predict the existence of a very large PCE when the external stress acts along the orthorhombic c -axis. Tensile stress destabilizes the AFE orthorhombic phase which results in a negative PCE. Compressive stress, on the other hand, further stabilizes the AFE phase and is associated with a positive PCE. The coexistence of both positive and negative PCE in the same material is very attractive for potential application as it allows to enhance the overall caloric response. We believe that our study is particularly timely in the light of the recent discovery of giant electrocaloric effect in PbZrO_3 [19] and may open a new direction in the area of functional materials.

Financial support for this work provided by the National Science Foundation Grant No. DMR-1250492 and MRI CHE-1531590.

-
- [1] V. K. Pecharsky and K. A. Gschneidner, Jr., *Phys. Rev. Lett.* **78**, 4494 (1997).
 - [2] A. de Campos, D. L. Rocco, A. M. G. Carvalho, L. Caron, A. A. Coelho, S. Gama, L. M. da Silva, F. C. G. Gandra, A. O. dos Santos, L. P. Cardoso, P. J. von Ranke, and N. A. de Oliveira, *Nature Mater.* **5**, 802 (2006).
 - [3] O. Tegus, E. Bruck, K. H. J. Buschow, and F. R. de Boer, *Nature* **415**, 150 (2002).
 - [4] J. Liu, T. Gottschall, K. P. Skokov, J. D. Moore, and O. Gutfleisch, *Nature Mater.* **11**, 620 (2012).
 - [5] L. Manosa, D. Gonzalez-Alonso, A. Planes, E. Bonnot, M. Barrio, J.-L. Tamarit, S. Aksoy, and M. Acet, *Nature Mater.* **9**, 478 (2010).
 - [6] L. Manosa, D. Gonzalez-Alonso, A. Planes, M. Barrio, J.-L. Tamarit, I. S. Titov, M. Acet, A. Bhattacharyya, and S. Majumdar, *Nature Commun.* **2**, 595 (2011).
 - [7] E. Bonnot, R. Romero, L. Mañosa, E. Vives, and A. Planes, *Phys. Rev. Lett.* **100**, 125901 (2008).
 - [8] A. S. Mischenko, Q. Zhang, J. F. Scott, R. W. Whatmore, and N. D. Mathur, *Science* **311**, 1270 (2006).
 - [9] B. Neese, B. Chu, S.-G. Lu, Y. Wang, E. Furman, and Q. Zhang, *Science* **321**, 821 (2008).
 - [10] W. N. Lawless, *Phys. Rev. B* **16**, 433 (1977).

- [11] Y. Bai, G.-P. Zheng, K. Ding, L. Qiao, S.-Q. Shi, and D. Guo, *J. Appl. Phys.* **110**, 094103 (2011).
- [12] S. Lisenkov and I. Ponomareva, *Phys. Rev. B* **86**, 104103 (2012).
- [13] S. Lisenkov, B. K. Mani, C.-M. Chang, J. Almand, and I. Ponomareva, *Phys. Rev. B* **87**, 224101 (2013).
- [14] Y. Liu, I. C. Infante, X. Lou, L. Bellaiche, J. F. Scott, and B. Dkhil, *Adv. Mater.* **26**, 6132 (2014).
- [15] A. Chauhan, S. Patel, and R. Vaish, *Appl. Phys. Lett.* **106**, 172901 (2015).
- [16] A. Chauhan, S. Patel, and R. Vaish, *Acta Mater.* **89**, 384 (2015).
- [17] K. M. Rabe, “Antiferroelectricity in oxides: A reexamination,” in *Functional Metal Oxides* (Wiley-VCH Verlag GmbH and Co. KGaA, 2013) p. 221.
- [18] R. Pirc, B. Roi, J. Koruza, B. Mali, and Z. Kutnjak, *Europhys. Lett.* **107**, 17002 (2014).
- [19] W. Geng, Y. Liu, X. Meng, L. Bellaiche, J. F. Scott, B. Dkhil, and A. Jiang, *Adv. Mater.* **27**, 3165 (2015).
- [20] B. K. Mani, S. Lisenkov, and I. Ponomareva, *Phys. Rev. B* **91**, 134112 (2015).
- [21] T. Yoshida, Y. Moriya, T. Tojo, H. Kawaji, T. Atake, and Y. Kuroiwa, *J. Therm. Anal. Calorim.* **95**, 675 (2009).
- [22] G. A. Samara, *Phys. Rev. B* **1**, 3777 (1970).
- [23] S. Sawai and H. Tanaka, *J. Korean Phys. Soc.* **51**, 758 (2007).
- [24] R. W. Whatmore and A. M. Glazer, *J. Phys. C* **12**, 1505 (1979).
- [25] I. Ponomareva and S. Lisenkov, *Phys. Rev. Lett.* **108**, 167604 (2012).
- [26] Y. Bai, G. Zheng, and S. Shi, *Appl. Phys. Lett.* **96**, 192902 (2010).
- [27] R. Herchig, C.-M. Chang, B. K. Mani, and I. Ponomareva, *Sci. Rep.* **5**, 17294 (2015).
- [28] A. Tishin and Y. Spichkin, *The magnetocaloric effect and its applications* (IOP Bristol and Philadelphia, 2003).
- [29] VidBobnar, ZdravkoKutnjak, and AdrijanLevstik, *Jpn. J. Appl. Phys.* **37**, 5634 (1998).
- [30] S. Yuce, M. Barrio, B. Emre, E. Stern-Taulats, A. Planes, J.-L. Tamarit, Y. Mudryk, K. A. Gschneidner, V. K. Pecharsky, and L. Maosa, *Appl. Phys. Lett.* **101**, 071906 (2012).
- [31] A. Roy Chaudhuri, M. Arredondo, A. Hähnel, A. Morelli, M. Becker, M. Alexe, and I. Vrejoiu, *Phys. Rev. B* **84**, 054112 (2011).

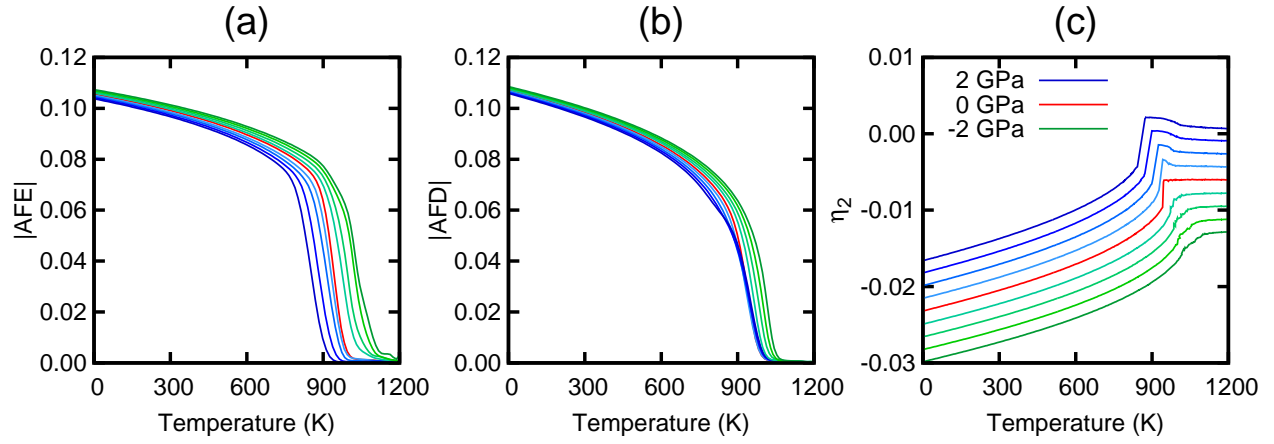


FIG. 1. Dependence of the magnitude of the AFE and AFD order parameters [(a) and (b)] and strain (c) on the temperature in the presence of different external stresses σ_2 .

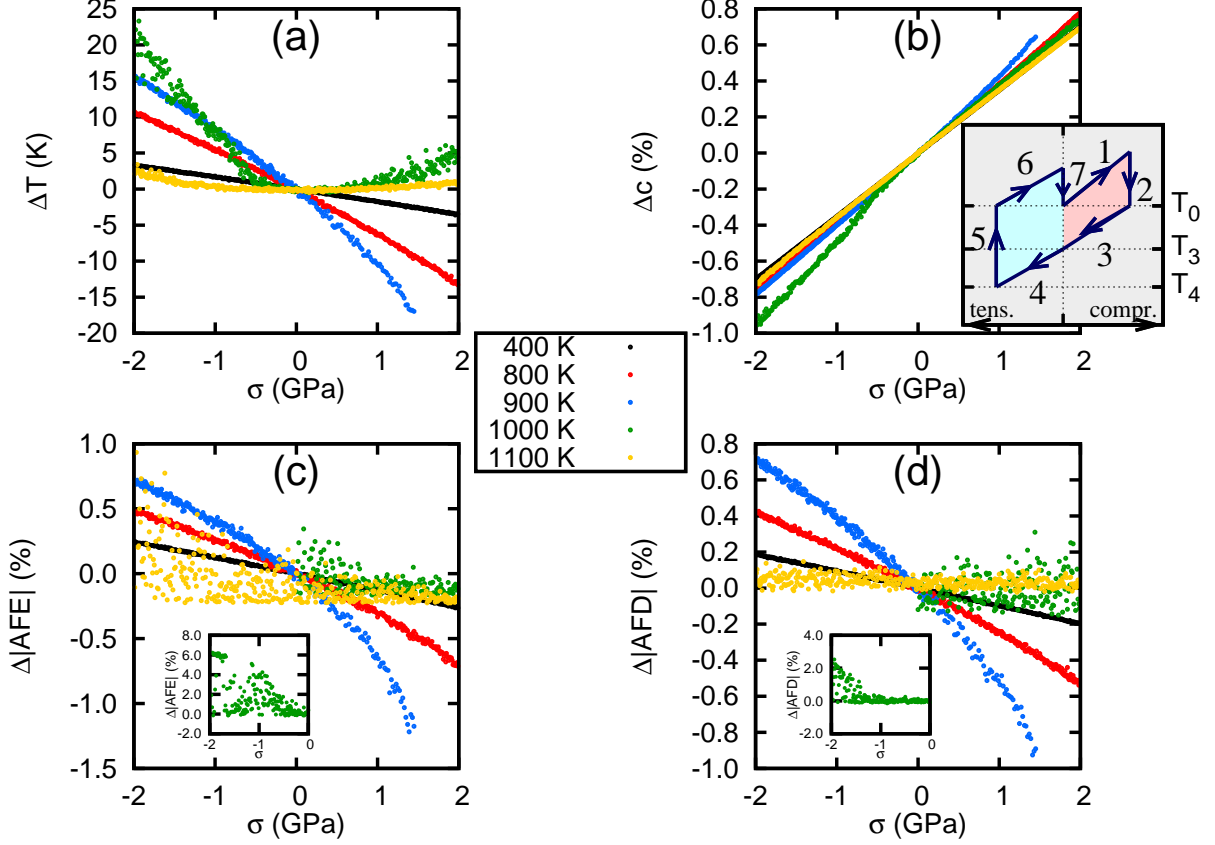


FIG. 2. (a) Dependence of the piezocaloric change in temperature on the applied stress. Dependence of the change in the c lattice constant (b), the magnitude of the AFE (c), and AFD (d) order parameters on the applied stress. The stress acts on the ab orthorhombic plane. The inset to panel (b) shows a basic refrigeration cycle that utilizes both positive and negative PCE. The cycle begins (step 1) with application of compressive stress which is followed by a heat exchange with a heat sink under constant stress (step 2). At step 3 the compressive stress is removed adiabatically resulting in a drop in the temperature below T_0 via positive PCE. At step 4 a tensile stress is applied producing an additional drop in the temperature via negative PCE. At step 5 the system returns to the original T_0 by absorbing the heat from the load. The cycle closes via an adiabatic removal of the tensile stress (step 6) followed by the heat exchange with the heat sink (step 7). The $\Delta T = T_4 - T_0$ of the double cycle exceeds that of a single cycle which utilizes either positive PCE ($\Delta T = T_3 - T_0$) or negative PCE ($\Delta T = T_4 - T_3$).

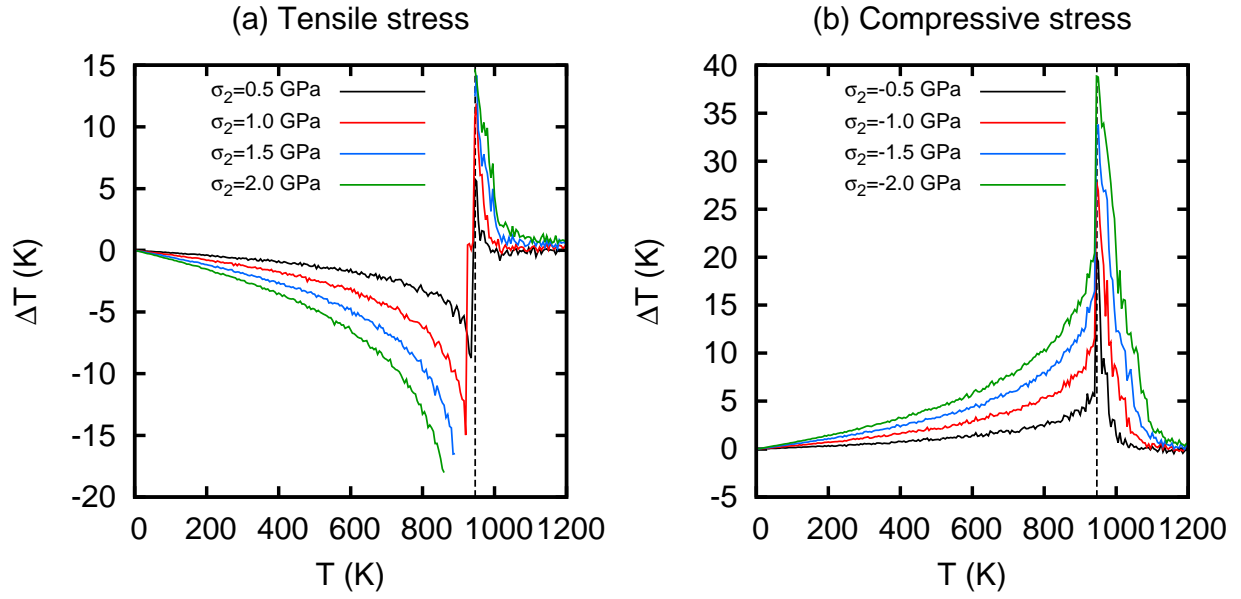


FIG. 3. Dependence of the piezocaloric ΔT on the temperature. Vertical lines indicate computational transition temperature.

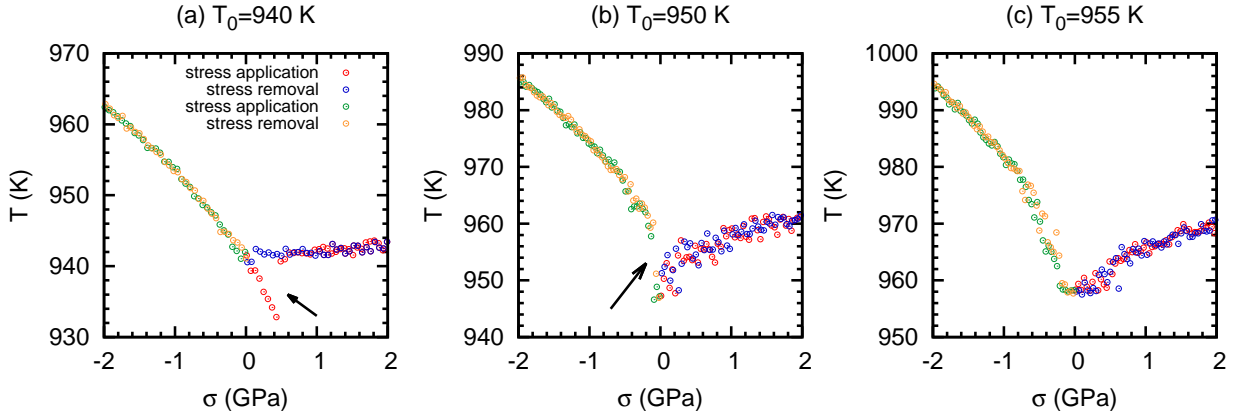


FIG. 4. Dependence of the temperature on the applied stress in the vicinity of the Curie point. (a), (b) and (c) give data for initial temperatures of 940 K, 950 K, and 955 K, respectively. Arrows indicate first-order phase transitions. Under tensile stress the first-order phase transition is irreversible and associated with hysteresis (see panel (a)).

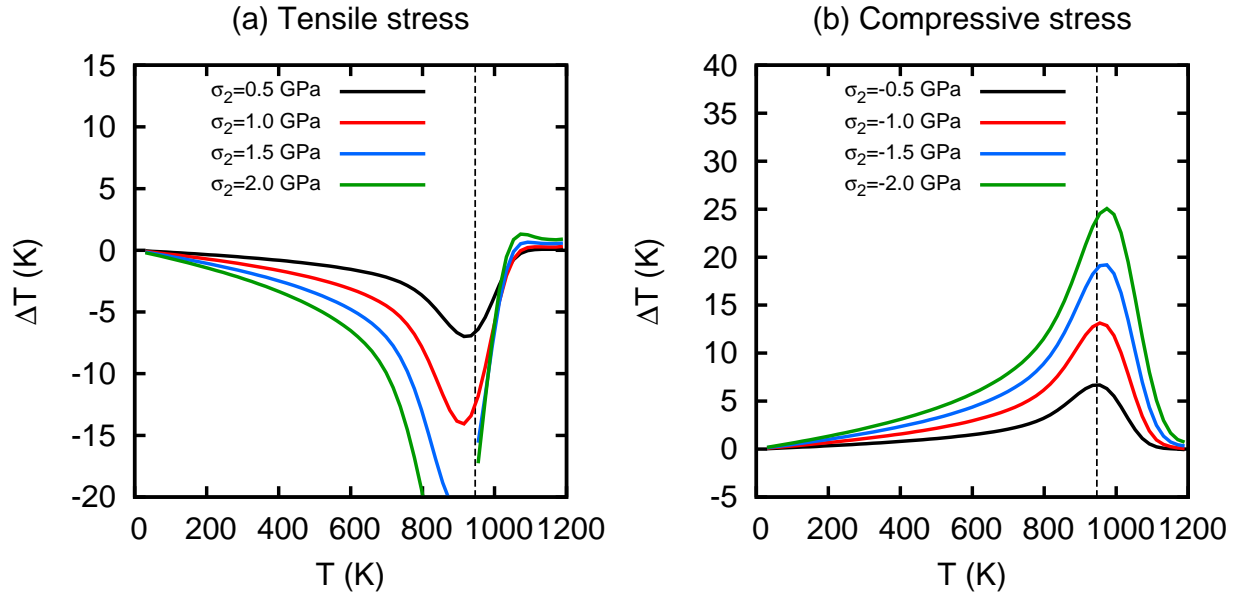


FIG. 5. Dependence of the piezocaloric ΔT on the temperature computed using the indirect approach. Vertical lines indicate computational transition temperatures. We removed the points associated with the irreversible phase transition.

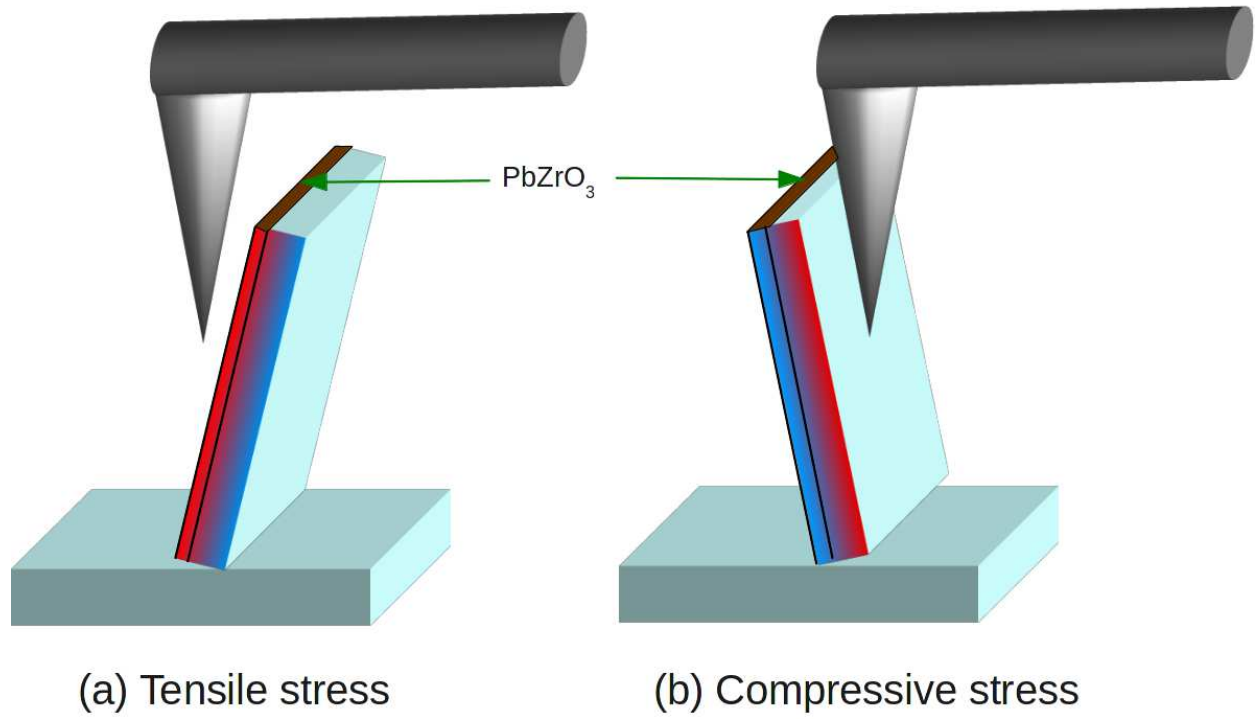


FIG. 6. Schematic view of the bending setup for experimental demonstration of PCE. The red and blue color schematically indicate tensile and compressive stresses, respectively, that develop in the structure upon bending.